Suppression of scattering in quantum confined 2D helical Dirac systems

J. Dufouleur, E. Xypakis, B. Buchner, Romain Giraud, J. Bardarson

Suppression of scattering in quantum confined 2D-helical Dirac systems

J. Dufouleur,[1,2,*] E. Xypakis,[3] B. Büchner,[1,4] R. Giraud,[5,6] and J. H. Bardarson[3,7]

[1] *Leibniz Institute for Solid State and Materials Research IFW Dresden, P.O. Box 270116, D-01171 Dresden, Germany*
[2] *Center for Transport and Devices, TU Dresden, D-01069 Dresden, Germany*
[3] *Max-Planck-Institut für Physik Komplexer Systeme, D-01187 Dresden, Germany*
[4] *Department of Physics, TU Dresden, D-01062 Dresden, Germany*
[5] *IFW Dresden, P.O. Box 270116, D-01171 Dresden, Germany*
[6] *INAC-SPINTEC, Univ. Grenoble Alpes/CNRS/CEA, 17 Avenue des Martyrs, F-38054 Grenoble, France*
[7] *Department of Physics, KTH Royal Institute of Technology, Stockholm, SE-106 91 Sweden*

(Dated: September 4, 2017)

Transport properties of disordered quantum confined helical Dirac systems are investigated in the large energy limit. As long as the 2D transport length is larger than the perimeter of the nanowire, the conductance and the Fano factor are sensitive to disorder only when the Fermi energy is close to an opening of a transverse mode. In the limit of a large number of transverse modes, transport properties are insensitive to the geometry of the nanowire or the nature and strength of the disorder but, instead, are dominated by the properties of the interface between the ohmic contact and the nanowire. In the case of a heavily doped Dirac metallic contact, the conductance is proportional to the energy with an average transmission $\mathcal{T} = \pi/4$ and a Fano factor of $F \simeq 0.13$. Those results can be generalized to a much broader class of contacts, the exact values of $\mathcal{T}$ and F depending on the model used for the contacts. The energy dependence of Aharonov-Bohm oscillations is determined, when a magnetic flux is threaded through the cross section of the nanowire.

Transport properties of two dimensional helical Dirac fermions were first studied in carbon nanotubes[1–5] and more recently in graphene[6,7] and topological insulators[8]. For massless fermions, the linear dispersion relation and the symmetries that constrain scattering not to connect orthogonal (pseudo)spins, induce a strongly anisotropic scattering, leading to a large transport scattering time[9–12]. The long length scale for the transport length ℓ results in large conductivities and in quantum confinement effects in disordered systems with one or more dimensions smaller than ℓ. Prior work[6,7] highlighted for instance the properties of Dirac fermions either in absence of quantum confinement[9,10] or disorder[13–15] or in presence of both but focusing on low energy[1–3,8,16,17]. Although the transport properties are roughly understood close to the Dirac point, the coexistence of strong quantum confinement and low Fermi energy in Dirac fermion system is rarely realized in real systems like 3D topological insulator nanowires[18,19] or narrow graphene nanoribbons[20–22].

A clear understanding of the interplay between scattering and quantum confinement at large Fermi energies would shed light on recent experimental works[18,19,23–27]. In particular, accounting for both contacts and disorder allows us to evaluate their relative contributions to the transport properties. Moreover, in the case of weakly disordered topological insulator nanowires, we provide the energy dependence of Aharonov-Bohm oscillations close to and far from the Dirac point. This makes it possible to distinguish topologically trivial features from nontrivial ones[18,19,26].

In this work, more specifically, we investigate the properties of disordered topological insulator nanowires with $\ell/W > 1$ where W is the perimeter of the nanowire. We consider the case of a perfect interface with metallic electrodes and we focus on the high-Fermi-energy regime ($\varepsilon \gg \Delta$ with $\Delta = hv/W$ and v the Fermi velocity) in the presence of a magnetic field parallel to the nanowire axis. Starting from an approximate analytical derivation of the transmission of transverse modes, we calculate the transport properties at any energy and magnetic flux, including quantum corrections induced by intermode scattering. Comparison with a numerical simulation validate our analytical approach and an excellent agreement is found at high energy as long as $\ell/W > 1$. In this regime, the energy and disorder strength dependence of the conductance and shot noise reveal the ballistic nature of the transport. Finally, we generalize our study to the case where a magnetic flux is thread through the cross section of the nanowire, leading to Aharonov-Bohm oscillations of the conductance.

I. MODEL

We consider the case of a band structure with a single spin-helical Dirac cone (Fig. 1a), as realized for example in Bi_2Se_3[28], but our results are easily generalized to the case of graphene nanoribbons or carbon nanotubes in absence of intervalley scattering. The system is described by the Dirac Hamiltonian

$$\mathcal{H} = v\mathbf{p}\cdot\boldsymbol{\sigma} + V(\mathbf{r}) + V_c \tag{1}$$

with $\boldsymbol{\sigma} = (\sigma_x, \sigma_y)$ the Pauli sigma matrices, $\mathbf{r} = (x, y)$ where x is the longitudinal coordinate and y the transverse coordinate, and $V(\mathbf{r})$ stands for a Gaussian corre-

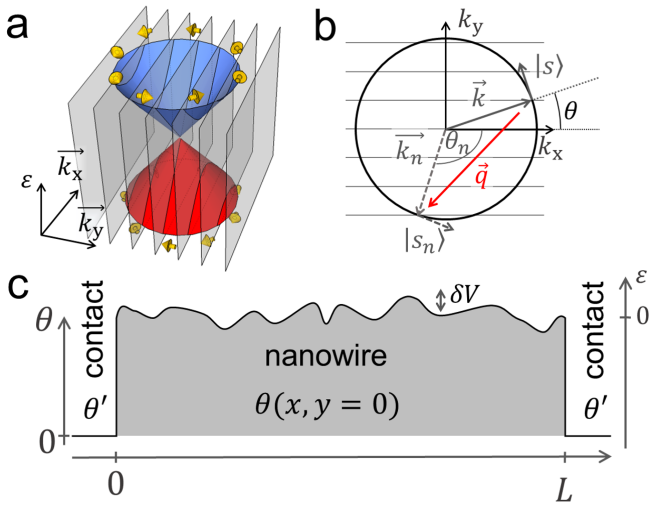

FIG. 1. a) 2D band structure of a massless fermion system with spin-momentum locking. The planes correspond to the section of the cone for discrete values of the transverse wave vector due to quantum confinement. b) section of the 2D band structure at a given Fermi energy. c) 1D cut of the disorder and contact potential at $y = 0$, plotted together with the corresponding θ angle.

lated scalar disorder such that

$$\langle V(\mathbf{r})V(\mathbf{r}')\rangle = g\frac{(\hbar v)^2}{2\pi\xi^2}e^{-|\mathbf{r}-\mathbf{r}'|^2/2\xi^2}. \tag{2}$$

Here ξ is the disorder correlation length and g is a dimensionless parameter that measures the disorder strength. The qualitative results of our study do not depend strongly on the exact nature of the disorder correlation function. The contacts are modeled by a potential $V_c \to -\infty$ for $x < 0$ and $x > L$ and $V_c = 0$ otherwise[13,16] (see Fig. 1c). This model corresponds to a strong doping of the topological insulator below metallic electrodes, or, equivalently, to the injection of quasiparticles from a metallic electrode with $k_x \gg k_y$ (k_x and k_y are the component of the wave vector $\mathbf{k}$ parallel and perpendicular to the axis of the nanowire). Our results, as we we will see below, can be generalized to a broader class of contacts.

In a nanowire geometry, k_y is quantized due to periodic boundary conditions (Fig. 1a and b). In general, $k_{\perp,n} = \varepsilon_n/\hbar v = (n + \phi/\phi_0 - 1/2) \times \Delta/\hbar v$ where the $1/2$ comes from the Berry phase induced by spin-momentum locking[29–31] (absent in graphene nanoribbons), $n \in \mathbb{Z}$ is a mode index, ϕ is the magnetic flux threaded through the cross section of the nanowire, $\phi_0 = h/e$ is the magnetic flux quantum and ε_n is the energy of the mode n. In addition to the transverse quantized energy Δ, we also consider the longitudinal quantized energy $\Delta_\parallel = \pi\hbar v/L$ where L is the length of the wire.

Ignoring first the quantum confinement and considering the 2D limit only, the transport relaxation time τ and the transport length $\ell = v\tau$ can be explicitly determined for a Gaussian potential, starting from Fermi's golden rule[16,32]. As expected, ℓ and τ do not depend on the incident direction of the $\mathbf{k}$-vector of the wave function[33]:

$$\ell = v\tau = \frac{2k\xi^2}{g}\frac{\exp(k^2\xi^2)}{I_1(k^2\xi^2)} \tag{3}$$

where I_1 is the modified Bessel function of the first kind. Even if the 2D limit is valid only for $k\ell \gg 4\pi$, such that the divergence of ℓ at low energy is smoothed out, ℓ reaches a minimum ℓ_m at energy ε corresponding to $k\xi \sim 1$. As a result, for a conductor with a finite width $W < \ell_m$, the disorder is not strong enough to set the system in the 2D diffusive limit. Boundary conditions then modify the density of states that exhibits a maximum at each transverse mode opening, a feature typical of the 1D nature of the subband associated to the mode—the system is then quantum confined. This condition reads $g \lesssim 0.5$ for $\xi/W = 0.05$ (see Appendix A).

II. TRANSMISSION MODES AND DISORDER

At high energies, ℓ is larger than the system size and transport properties are determined by the interface between the nanowire and the lead. A perfect interface simply consists of a step in the chemical potential at $x = 0$ and $x = L$. As long as the step does not depend on y, translational invariance implies the conservation of k_y such that only intra-mode backscattering processes takes place at the interface. Each transverse mode can be considered independently following Refs. 13 and 34. For a given mode n with $\theta = \arctan([(\varepsilon/\varepsilon_n)^2 - 1]^{-1/2})$, the reflection ($r_{\theta',\theta}$) and transmission ($t_{\theta',\theta}$) coefficients only depend on θ in the nanowire and θ' in the contact. Contrary to the massive case, the Hamiltonian (1) does not require the continuity of the spatial derivative of the wave function but rather only the continuity of the two-component wave function, which gives $r_{\theta',\theta} = \sin([\theta - \theta']/2)/\cos([\theta + \theta']/2)$ and $t_{\theta',\theta} = \cos(\theta')/\cos([\theta + \theta']/2)$. The total transmission amplitude t of the mode n considering a non-disordered nanowire and two contacts with perfect interfaces is

$$t = \frac{\cos\theta\cos\theta'}{\cos\theta\cos\theta'\cos\varphi + i\,(\sin\theta\sin\theta' - 1)\sin\varphi} \tag{4}$$

with $\varphi = k_x L$. This expression is a generalization to an arbitrary θ' of the transmission amplitude for propagating modes found in Ref. 13 (where $\theta' = 0$). Contrary to Ref. 13, we do not consider evanescent modes which exponentially vanish far from the Dirac point and for long distances between the contact ($L > W$) such that transport properties are strongly dominated by propagating modes. The transmission is $T = |t|^2$.

We first consider a weak disorder and follow a Wentzel-Kramers-Brillouin approach[35]. The main effect of the disorder is to randomly redistribute the phase φ of each mode without inducing any inter-mode scattering. Thus, the position of the Fabry-Pérot resonances that corresponds to $k_x L = p\pi$ ($p \in \mathbb{N}$) in the clean case will

be shifted depending on the disorder configuration and the disorder-averaged transmission is given by $\langle T\rangle = 1/2\pi \times \int_0^{2\pi} |t(\varphi)|^2\, d(\varphi)$. This approach is equivalent to a temperature smearing with $4k_BT > \Delta_\parallel$. $\langle T\rangle$ can be explicitly calculated:

$$\langle T\rangle = \frac{\cos\theta\cos\theta'}{1-\sin\theta\sin\theta'}. \quad (5)$$

More particularly, when $V_c \to -\infty$ we have $\theta' \simeq 0$ and

$$\langle T\rangle = \cos\theta = \sqrt{1-\left(\frac{\varepsilon_n}{\varepsilon}\right)^2}. \quad (6)$$

We note that the transmission of a mode differs from 1 except for $\theta = 0$ that corresponds to the perfectly transmitted mode discussed in[16,36,37]. This mode corresponds to $\varepsilon_n = 0$ which requires half a quantum of flux to be threaded through the cross-section of the nanowire to compensate the Berry phase picked up by a particle when it goes around the nanowire. This approach is valid as long as (i) the system is quantum confined, which requires $\ell > W$ and (ii) $|d\lambda/dx| \ll 2\pi$ where $\lambda = 2\pi/k_x$[35]. It is therefore not valid close to the onset of a mode but it is satisfied for $\varepsilon \gtrsim \varepsilon_n$ for the conditions we are using here.

We compare the analytical expression (6) to numerical simulations following the method presented in[16,38,39]. The transmissions of a disordered nanowire with $W =$ 200 nm and $L = 500$ nm is calculated up to $\varepsilon/\Delta \sim 25$ and averaged over $\sim 10^3$ disorder configuration for different strength of disorder ranging from the ballistic limit ($g = 0$) to the diffusive limit ($g = 1$). We choose a correlation length $\xi = 10$ nm consistent with experimental measurements[12].

Results are presented in Fig. 2 for half a flux quantum threading the cross section of the nanowire. Due to time reversal symmetry, the zero energy mode is topologically protected and its transmission is equal to 1 independently of the strength of the disorder[16,37]. All other modes exhibit Fabry-Pérot resonances that are not fully averaged out for a weak disorder ($g \lesssim 0.02$). Nevertheless, the average transmission roughly follows the analytical formula (6) in general.

We notice two kinds of deviation from the adiabatic limit for the simulated data. Firstly, dips appears close to the onset of each mode for $g \gtrsim 0.05$. They are smeared out for $g \gtrsim 1$. This is the signature of the modification of the density of states by quantum confinement. More quantitatively, starting from the Fermi golden rule and assuming $\ell > W$, we obtain:

$$\frac{1}{\tau_{\mathbf{k}}} = \frac{gv}{2W}\sum_{\mathbf{k}_n}\left|\frac{1-\cos^2\theta_q}{\cos\theta_n}\right|\exp\left(-\frac{q^2\xi^2}{2}\right) \quad (7)$$

where $\tau_{\mathbf{k}}$ is the transport time of a $\mathbf{k}$-state, $\mathbf{q} = \mathbf{k}_n - \mathbf{k}$, θ_n is the angle of final $\mathbf{k}_n$-state and $\theta_q = \theta - \theta_n$. Contrary to the diffusive case, $\tau_{\mathbf{k}}$ explicitly depends on the initial state $\mathbf{k}$. Dips in the transmission come from the opening of transverse mode associated to the divergence of the 1D density of state ($\cos\theta_n = 0$). Far from the onset ($\varepsilon - \varepsilon_n \gg \Delta$), this effect is strongly reduced by the exponential cut-off of the Gaussian disorder ($q^2\xi^2/2 \gg 1$). For $g \gtrsim 1$, the disorder broadening induces overlapping dips and the transmission deviates clearly from its ballistic limit (see Fig. 2c).

Secondly, at high energy, the transmission is above the ballistic limit for any value of g. We attribute this to an interplay between the contact and the disorder due to weak anti-localization when inter-mode scattering is allowed as described in Ref. 2. The disorder induces a deviation from the ballistic transmission T_0 that takes into account quantum interferences in a given mode (Fabry-Pérot interferences) and we have generally $T = T_0 + \delta T$ with $\delta T/T_0 \ll 1$ for a weak disorder. We consider weak anti-localization type interferences between the two time reversal symmetric states $\mathbf{k}_+ = \mathbf{k}_y + \mathbf{k}_x$ and $-\mathbf{k}_+$. The ballistic transmission T_0 corresponds to a situation where only intra-mode scattering occurs (at the interface with the contact) with no inter-mode scattering. As a first approximation, we take into account processes involving only one inter-mode scattering event. The transmission T of a given mode corresponding to a perpendicular wave vector $\mathbf{k}_y$ relates the incoming plane wave ($\mathbf{k}_+ = \mathbf{k}_y + \mathbf{k}_x$) to the outcoming plane wave ($\mathbf{k}_- = \mathbf{k}_y - \mathbf{k}_x$) such that the two kind of interfering paths that lead to weak

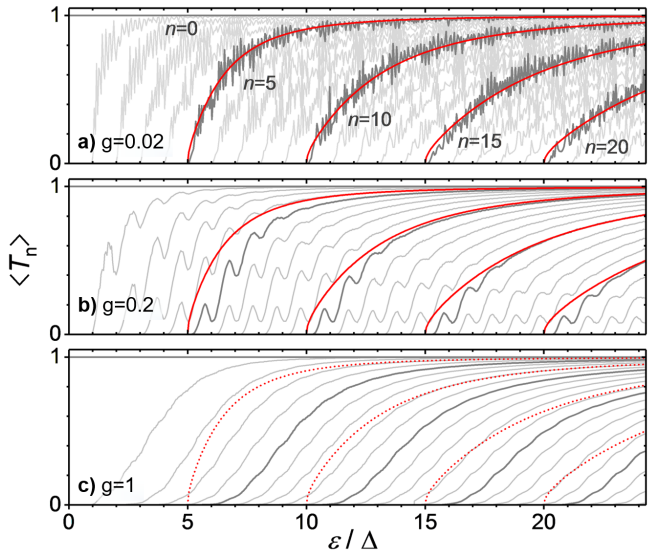

FIG. 2. The transmission of the transverse modes calculated and disorder-averaged for different disorder strength g (0, 0.02, 0.2 and 1) ranging from the ballistic to the diffusive regime. Black lines indicate the ballistic transmission with no quantum corrections ($\gamma_0 = \gamma_1 = 0$). Red lines are the best fit of the transmission with quantum corrections for a) and b) ($\gamma_0 = 0.39$ and 0.43 and $\gamma_1 = -0.80$ and -0.92 for $g = 0$ and $g = 0.02$ respectively). Good agreement with numerical data with $\gamma_0 = 0.4$ and $\gamma_1 = -0.85$ for $g = 0.2$ is seen, whereas no satisfactory parameters fit the $g = 1$ data; the $\gamma_0 = 0.4$ and $\gamma_1 = -0.85$ transmissions are indicated by dotted lines.

anti-localization can be described by the two following scattering sequences: $\mathbf{k}_+ \to \mathbf{k}_- \to -\mathbf{k}_+ \to \mathbf{k}_-$ and $\mathbf{k}_+ \to -\mathbf{k}_- \to -\mathbf{k}_+ \to \mathbf{k}_-$ (see Fig. 3). Due to the π Berry phase that a particle picks up along a backscattering loop associated to a 2π rotation of the spin, the correction contribute to an enhancement of the transmission at high energy for quantum confined spin-helical Dirac systems[2]. Such scattering events involve both adiabatic backscattering at the contact interface ($\mathbf{q}_1 = -2\mathbf{k}_\mathrm{x}$) and inter-mode scattering on the disorder ($\mathbf{q}_2 = -2\mathbf{k}_\mathrm{y}$), which limits the corrections to small $\|\mathbf{q}_2\| < 1/\xi$ due to the cutoff of the disorder in the formula (2). The $\mathbf{q}_1$-scattering process is related to the reflection coefficient $|r| = |\sin\theta/(1+\cos\theta)| \simeq |\sin\theta|$ for small θ. Therefore the first order correction due to weak anti-localization is $\propto (\sin\theta)^2 = (\varepsilon_\mathrm{n}/\varepsilon)^2$. In general, higher order are proportional to $(\varepsilon_\mathrm{n}/\varepsilon)^{2p}$ with $p \in \mathbb{N}$ and the transmission of the n^{th}-mode including the quantum corrections can be written as

$$\langle T\rangle = \cos\theta \times \left(1 + \sum_{p=0}^{\infty} \gamma_p \left(\frac{\varepsilon_n}{\varepsilon}\right)^{2(p+1)}\right) \tag{8}$$

In general, the coefficients γ_p depend on the effectiveness of the disorder in coupling $\mathbf{k}_+$ to $-\mathbf{k}_-$. We find good agreement with the numerical simulation by including only first two order corrections γ_0 and γ_1, see Fig. 1, for the full set of transmissions up to $g = 0.5$ at high energy.

Importantly, γ_0 and γ_1 only weakly depend on L, ξ and γ_0 as long as $\ell > W$ (see Appendix B) with $\gamma_0 \approx 0.43$ and $\gamma_1 \approx -0.93$. Hence, transport properties of the system depend neither on the length nor on the detail of the microscopic disorder (g and ξ) anymore.

III. CONDUCTANCE AND SHOT NOISE

From the transmissions of the different transverse modes, we extract the conductance $G = e^2/h \times \sum_i \langle T_i\rangle$ and the Fano factor $F = \sum_i \langle T_i\rangle(1-\langle T_i\rangle)/\sum_i \langle T_i\rangle$ for a quantum confined nanowire. For a large number of modes ($\varepsilon \gg \Delta$), we can take the continuous limit and we replace the discrete sum by an integral where i is considered as an continuous index. Keeping only γ_0 and γ_1 corrections, we have

$$G = \frac{e^2}{h}\frac{2\varepsilon}{\Delta}\mathcal{T}, \tag{9}$$

$$F = 1 - \left(\frac{2}{3} + \frac{4}{15}\gamma_0 + \frac{4}{35}\gamma_1\right)/\mathcal{T} \tag{10}$$

with the average transmission per transverse mode

$$\mathcal{T} = \frac{\pi}{4} + \frac{\pi}{32}(2\gamma_0 + \gamma_1). \tag{11}$$

Agreement with the simulations is excellent for $g < 0.05$ even at low energy and it remains very good up to $g \simeq 0.5$ in the limit of large number of modes. We note that for all g, best fits gives $2\gamma_0 \sim -\gamma_1$ such that the conductance and the Fano factor can be approximated by

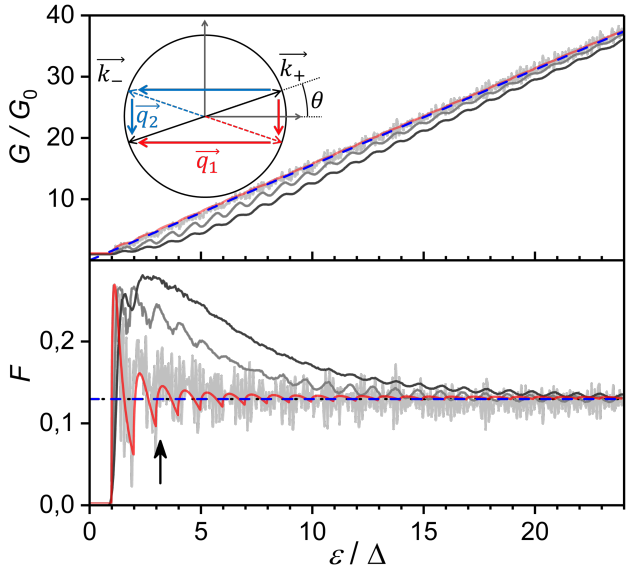

FIG. 3. Upper panel: Energy dependence of the conductance. Gray lines are numerical data for $g = 0.02$, 0.2 and 0.5 (from light to dark gray). The red line is the conductance calculated from Eq. (9) with $\gamma_0 = 0.43$ and $\gamma_1 = -0.92$ and blue dashed line is the large number of mode limit for the same values of γ_0 and γ_1. A schematic of a WAL backscattering process is shown in the inset. Lower panel: Energy dependence of the Fano factor shown with the same color code as for the conductance. The ballistic limit ($\gamma_0 = \gamma_1 = 0$) is indicated by the dotted line and the arrow points at the energy corresponding to $k\xi = 1$.

$$G \simeq \frac{e^2}{h}\frac{2\varepsilon}{\Delta}\frac{\pi}{4} \tag{12}$$

$$F \simeq 1 - \frac{8}{3\pi} \tag{13}$$

As already reported for graphene nanoribbons[21,22], the linear dependence of the conductance with ε or k_F is an indication of quantum confinement. In our case the proportional factor is $\mathcal{T} = \pi/4$ instead of 1 when the coupling to the contact is perfect. Generally, the transmission of a mode $\langle T\rangle$ depends on the model used for the contact far from the Dirac point[40–42]. Nevertheless, as long as the transmission (t) and reflection (r) coefficients of the contact-to-nanowire junction are functions of the energy through the ratio $\varepsilon/\varepsilon_n$ only, the high energy conductance and the Fano factor can be expressed in a similar way to that in Eq. (12) and Eq. (13). Indeed, the transmission $\langle T\rangle$ is then also a function of $\varepsilon/\varepsilon_n$ and if we note $\langle T\rangle = f(\varepsilon_n/\varepsilon)$, we have

$$G \simeq \frac{e^2}{h}\frac{2\varepsilon}{\Delta}\int_0^1 f(x)dx, \tag{14}$$

$$F \simeq 1 - \frac{\int_0^1 (f(x))^2\,dx}{\int_0^1 f(x)dx}. \tag{15}$$

The average transmission is given by $\mathcal{T} = \int_0^1 f(x)dx$. In the model we used so far, this condition is satisfied as long as we neglect intermode scattering.

We can now examine the conditions related to the energy dependence of t and r depending on the model for the contact. We focus here on Dirac type contact for any value of V_c and on a (massive) metallic contact and determine the energy dependence of t and r, with the Fermi energy in the contact a constant. This corresponds to the real situation of a gated device for which the field effect is screened under the contact and not in the nanowire. We consider the case of a perfect interface which induces no intermode scattering ($\partial V_c/\partial y = 0$).

For a contact modeled by a highly doped Dirac fermions, the global transmission between a mode defined by any θ' in the contact and θ in the nanowire is given by Eq. (5). As a result, $\langle T\rangle$ depends on the energy ε through $\cos\theta$ and $\sin\theta$ that depend on $\varepsilon/\varepsilon_n$ only so that the previous condition is satisfied.

For a massive contact, each transverse mode is spin degenerate and the nanowire acts as a perfect spin filter: only the spin oriented along θ is transmitted, the orthogonal spin being completely reflected. The transmission properties of the quasi-particle are then given by the continuity of wave function and its spatial derivative as for massive particles only. The transmission and reflection coefficient between the contact and the nanowire are now given by $t = 2k_x/(k_x + k'_x)$ and $t = (k_x - k'_x)/(k_x + k'_x)$. Taking into account the conservation of k_y at the interface, we have $k_x \tan\theta = k'_x \tan\theta'$. Hence, t and r again depend on ε through the ratio $\varepsilon/\varepsilon_n$ only and following the method developed above for Dirac contact, we can show that $\langle T\rangle = 2\tan\theta\tan\theta'/(\tan^2\theta + \tan^2\theta)$. Again, this expression satisfies the energy dependence condition.

From Eq. (14) and (15), we observe that the exact nature of the contact influences the slope of the energy dependence of the conductance and the high energy limit of the Fano factor. We focus below on the effect of disorder in the nanowire. For strong values of the disorder strength, the worst agreement is found when $k\xi \sim 1$ which roughly corresponds to $\ell \approx \ell_m$ (see Fig. 3). There, deviations to the weak disorder regime are related to intermode scattering that induces dips in the mode transmissions as shown in Fig. 2. Those dips are responsible for the oscillations in $G(\varepsilon)$.

Remarkably, the transport properties strongly deviate from the diffusive limit, for which $G \propto g^{-1}$ and $G \propto L^{-1}$ (see Appendix C). For $\ell > W$, scattering to modes close to their onset dominates [Eq. (7)], inducing oscillations of the transmission. As long as the disorder broadening $\delta = h/\tau$ is smaller than Δ, scattering only has marginal effect on G since the nonoverlapping condition $\Delta/\delta = \ell/W > 1$ holds for any mode index and therefore over the full energy scale. Hence, quantum confinement drives the system in the ballistic regime. This weakening of the scattering by the quantum confinement leads to a conductance that is not proportional to the length between the contact as observed in Ref. 18. The ballistic feature of the conductance is confirmed by the low value of F that is significantly smaller than its diffusive value $F = 1/3$ at large energy (see Fig. 3). This value is given by the nature of the interface between the nanowire and the contact. In the case of a perfect transmission of the interface like for a quantum point contact geometry[20–22], the Fano factor should vanish. For the perfect interface considered here, the transmission of each mode is not equal to 1 but F is nevertheless considerably reduced with respect to its diffusive limit.

The consequences of the quantum confinement on the transport regime are specific to Dirac systems. For massive particles with mass m, the quantum confinement condition reads $\ell/W \simeq \Delta_0 N/\delta > 1$ where N is the number of transverse modes and $\Delta_0 = \pi^2\hbar^2/(mW^2)$. As the energy spacing between the modes n and $n+1$ is $\simeq n\Delta_0$ for $n \gg 1$, the quantum confinement condition at large energy ($N \gg 1$) does not guarantee the non-overlapping between two consecutive transverse modes, especially for small index modes ($n \simeq 1$). As a result strong deviation from the ballistic regime is expected for massive particles even for $\ell \gtrsim W$.[43]

IV. AHARONOV-BOHM OSCILLATIONS

The influence of an Aharonov-Bohm flux on the transmission of the mode n is entirely contained in the value of ε_n. We neglect here the effect of a Zeeman coupling that only shifts the position of the Dirac point and renormalizes the value of the Aharonov-Bohm period. We use our model to extract the complete flux dependence of the conductance at low and large energy in the clean limit where intermode scattering is neglected ($g < 0.1$). As we can see in Fig. 4, the Aharonov-Bohm amplitude $\delta G(\varepsilon)$ is maximum at $\varepsilon = 0$ where $\delta G = e^2/h$. Close to $\varepsilon = \Delta/2$, δG drops down and oscillates in a sawtooth manner with a period $\Delta/2$ as experimentally observed in[18,26]. More information on the specific shape of the Aharonov-Bohm oscillations are given in Appendix D. Fig. 4 indicates that each period is associated to a π-phase shift which has been experimentally observed in Ref. 26. Such phase shifts are a consequence of the quantum confinement and has a trivial origin. Only the low energy pinning of δG at e^2/h for any values of g, L, W or ξ is a signature of the nontrivial topology.

V. CONCLUSION

In summary, we determined the transmission of any mode of a quantum confined Dirac nanowire including quantum correction in the presence of disorder and for a perfect interface with the contact. Our analytical analysis is in good agreement with numerical simulations and shows that quantum confinement ($\ell/W > 1$) drives the system into a ballistic regime, with an average transmission per mode of $\pi/4$ and a Fano factor $F \simeq 0.13$.

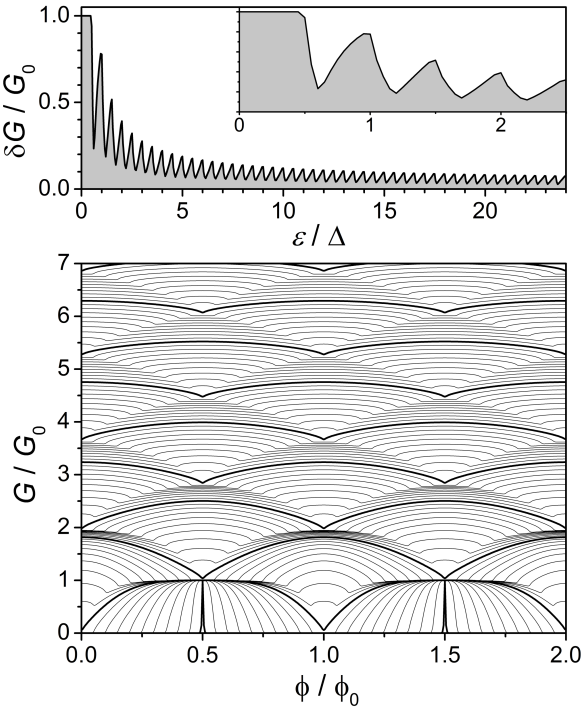

FIG. 4. Upper panel: Energy dependence of Aharonov-Bohm oscillations for $g = 0.02$ ($\gamma_0 = 0.43$ and $\gamma_1 = -0.92$) at a temperature $4k_BT/\Delta = 0.01$. The inset is a zoom closed to $\varepsilon/\Delta = 0$. Lower panel: the flux dependence of the conductance for different energy at the same temperature. The smaller value of the conductance corresponds to $\varepsilon/\Delta = 0$ and the larger one to $\varepsilon/\Delta = 4.5$ in steps of $\varepsilon/\Delta = 0.05$. Energies such that $2\varepsilon/\Delta \in \mathbb{N}$ are indicated with bold lines.

Aharonov-Bohm oscillations are found to be periodically modulated in energy with a period corresponding to $\Delta/2$. A phase shift of the oscillations occurs every time that the Fermi energy crosses an integer value of $\Delta/2$. At low energy ($\varepsilon < \Delta/2$), a signature of the topology can be seen in the amplitude of oscillations which saturates at e^2/h, independently of the geometry or the microscopic properties of the disorder.

Acknowledgments

J.D. gratefully acknowledges the support of the German Research Foundation DFG through the SPP 1666 Topological Insulators program. The DFG also supported this work through the Collaborative Research Center SFB 1143. This work was partially supported by the ERC starting grant QUANTMATT n°= 679722.

Appendix A: Energy dependence of ℓ/W

We present in Fig. 5 the energy dependence of ℓ/W. For Dirac fermions, the transport length ℓ has a minimum

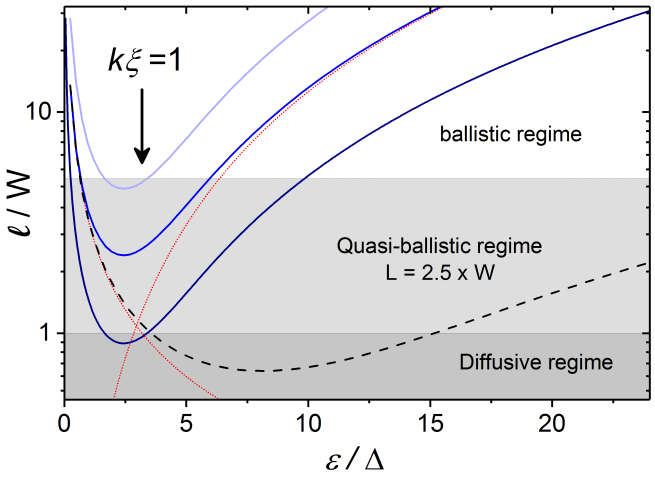

FIG. 5. Transport length ℓ as a function of energy ε for $\xi/W = 0.05$ and $g = 0.1$ (light blue), 0.2 (blue) and 0.5 (dark blue). Red dotted lines indicates the asymptotic dependence at low and high energies for $\xi/W = 0.05$ and $g = 0.2$. The black dashed line shows ℓ with $\xi/W = 0.015$ and $g = 0.2$. The gray domains indicate the ballistic regime characterized by $\ell > 2L$ with $L = 2.5 \times W$ and the quantum confined (quasi-ballistic) regime for which $\ell > W$.

ℓ_m for $k\xi \sim 1$ and diverges both at low energy (due to the reduction of the density of states) and at large energy (due to the anisotropy of scattering). In those two limits, ℓ can be approximated by its asymptotic form

$$\ell \sim \begin{cases} 4/(gk) & \text{for } k\xi < 1, \\ 2\sqrt{2\pi}k^2\xi^3/g & \text{for } k\xi > 1. \end{cases} \quad \text{(A1)}$$

This is different from the massive case for which $\ell \to 0$ at low energy. As the 2D approximation is only valid for $k\ell \gg 1$, the low energy divergence will be smoothed out.

In Fig. 5, the quantum confinement condition $\ell_m > W$ is satisfied for $g \lesssim 0.5$ for $\xi/W = 0.05$. We note that this approach does not describe collective effects like Thomas-Fermi screening. It is therefore not suitable for an accurate determination of the energy dependence of ℓ that requires to take into account the density dependence of both ξ and $\delta V = \hbar v/\xi\sqrt{g/2\pi}$[9,10]. Nevertheless, the aim of this work is to show that the transport properties of quasi-ballistic systems are dominated by the interface between the contact and the nanowire and not by the disorder in the nanowire, such that the exact energy dependence of ℓ does not play a role for our conclusions as long as $\ell_m \gtrsim W$.

The values of ℓ explain the clear ballistic features (Fabry-Pérot) observed for $g = 0.02$ (see Fig. 2a of the main text) since ℓ_m lies above the ballistic limit whereas those resonances are averaged out for $g = 0.2$ (see Fig. 2b of the main text), for which ℓ_m is below this limit. Nevertheless, the dips due to intermode scattering for $g = 0.2$ reveal the quantum confinement as expected since ℓ_m is above the diffusive limit for any ε. Finally, dips are smeared out by disorder broadening for $g = 1$ as shown

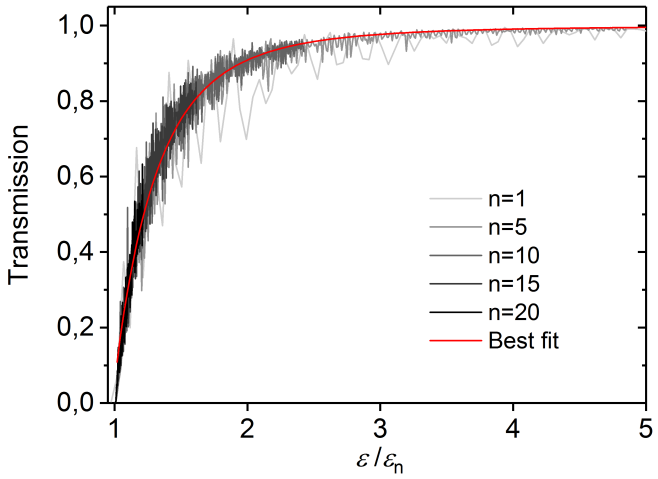

FIG. 6. The transmission for the modes corresponding to $n = 1$, 5, 10, 15 and 20 (from light gray to black) as a function of $\varepsilon_n/\varepsilon$ and for $g = 0.02$ and $L/W = 2.5$. The best fit corresponds to the red line.

in Fig. 2c, pointing to a diffusive regime as expected from ℓ_m that clearly lies below the diffusive limit in a broad range of energy.

Appendix B: Fit of the transmissions and dependence of the γ parameters

In order fit the transmissions of different modes to find the best γ parameters, we used the fact that the transmissions of the different transverse modes are depend on the ratio $\varepsilon_n/\varepsilon$ only for weak enough disorder. We plot the transmissions of the modes $n = 1$, 5, 10, 15 and 20 as a functions of $\varepsilon_n/\varepsilon$ in Fig. 6. We restrict our analysis to only five modes but no significant differences are obtained if all modes are taken into account. The transmissions are roughly superimposed and we fit the data with a single set of free parameters γ_0 and γ_1 that describe the quantum corrections for all transmissions. For systems close to the diffusive limit, we adjust the parameters to minimize the error in the high energy limit only, without applying the full fitting procedure. Agreement is found to be excellent over the full energy range for $g < 0.1$ (ballistic regime). At high energy ($\varepsilon/\varepsilon_n \gg 1$) excellent agreement can be found for g up to 0.5.

The dependence of the γ parameters on the disorder strength, wire length and correlation length is weak (see Fig. 7, which is plotted on a semi-logarithmic scale). Nevertheless, the dependence of the parameters corresponds to what is roughly expected. The longer the nanowire is, the stronger is the interaction with the disorder and the stronger should be the quantum corrections as reported by the dependence with L. Similar evolution is expected and observed for the g dependence. As explained in the main text, the ξ dependence leads to corrections that vanish for long ξ since the $\mathbf{q}_2$ scattering process exponentially decays with ξ. The scattering processes that lead to the first corrections of the transmission are indicated in the Fig. 8.

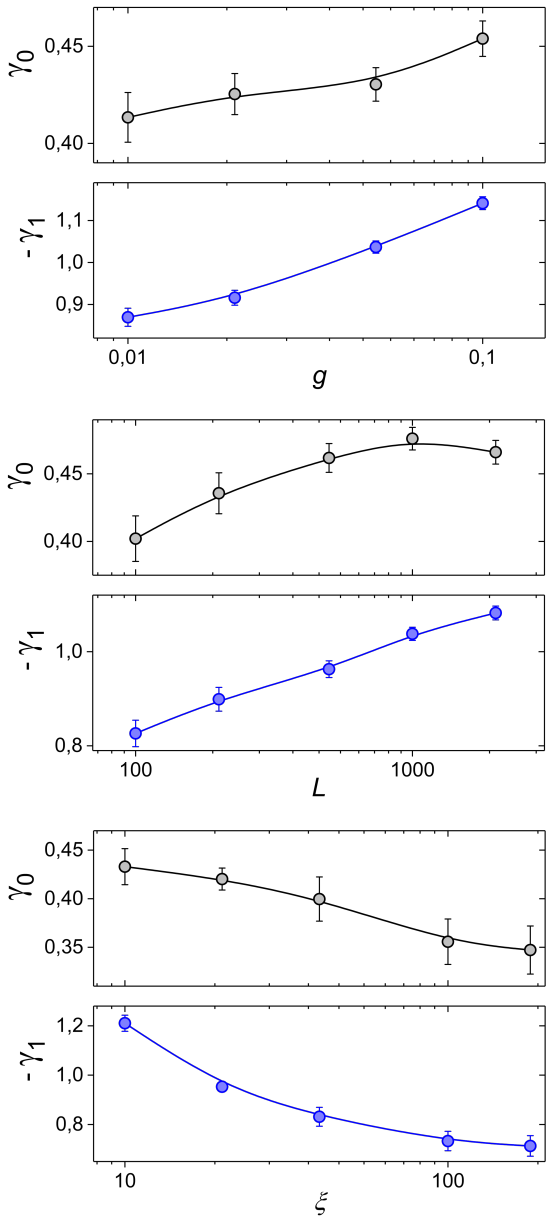

FIG. 7. The dependence of γ_0 and γ_1 is shown as a function of L, g and ξ in a semi-logarithmic graphs.

Remarkably, the ratio γ_0/γ_1 is almost constant for any value of the different parameters and we have $\gamma_1/\gamma_0 \simeq -2$. Hence, the contribution of the two first order transmission corrections to the transport properties compensate each other (see Eq. (9) and (10) in the main text) and the conductance as well as the Fano factor are very close to their pure ballistic limit.

Appendix C: Length dependence of the transport properties

We focus here on the length dependence of the transport properties (G and F) for $g = 0.02$ and $g = 0.2$ (Fig. 9). In the weak disorder limit ($g = 0.02$ in Fig. 9 left), the length has only a marginal effect on the conductance or the Fano factor. Generally, it induces sharp dips in the transmission (and then in the conductance) for each energy corresponding to the onset of a transverse mode that does not influence significantly the general transport properties. This is expected since for such a weak disorder, the system is in the ballistic regime ($\ell_m > 2L$) even for $L = 2$ μm (see Fig. 5).

For a stronger disorder ($g = 0.2$ in Fig. 9 right), the system is far below the ballistic limit for $L = 500$ nm to $L = 2$ μm and even very close to this limit for $L = 200$ nm. We indeed observe a length dependence of the conductance but this dependence is much weaker than in the diffusive regime, for which $G \propto 1/L$. Likewise, the Fano factor remains well below the diffusive limit($F = 1/3$), which confirms the ballistic nature of the transport even for large ratio L/W as long as the system is quantum confined.

Appendix D: Aharonov-Bohm oscillations

The Fig. 4 in the main text shows the expected shape of the Aharonov-Bohm oscillations for weakly disordered system where the magnetic flux dependence of δG is plotted for different positions of the Fermi energy. It indicates a rich content in harmonics of δG as observed in experiments[18,25]. At low energy ($\varepsilon \lesssim \Delta/2$), the conductance exhibits sharp peaks for $\phi = \phi_0/2$ and the Fourier transform of the magnetoconductance contents therefore many harmonics is particularly large. The harmonic content is strongly reduced when the energy increases but the ratio between the fundamental and the first harmonic remains generally energy dependent. Hence, this ratio is small for $2\varepsilon/\Delta \in \mathbb{N}$ whereas $2\varepsilon/\Delta + 1/2 \in \mathbb{N}$ is associated with a large resurgence of the second harmonic. It should be noticed that the presence of intermode scattering is expected to significantly modify the amplitude and the shape of the Aharonov-Bohm oscillations (less harmonics content) for rather strong disorder ($g > 0.1$).

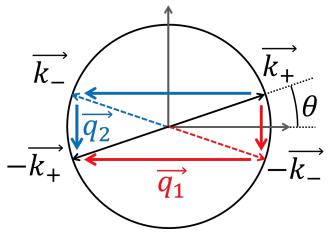

FIG. 8. Schematic describing weak-antilocalization implying reflection on the contact ($\mathbf{q}_1$) and disorder scattering ($\mathbf{q}_2$) in a quantum confined system.

* email: j.dufouleur@ifw-dresden.de

[1] T. Ando and T. Seri, Journal of the Physical Society of Japan **66**, 3558 (1997).
[2] T. Ando, T. Nakanishi, and R. Saito, *n*, Journal of the Physical Society of Japan **67**, 2857 (1998).
[3] T. Ando and T. Nakanishi, Journal of the Physical Society of Japan **67**, 1704 (1998).
[4] P. L. McEuen, M. Bockrath, D. H. Cobden, Y.-G. Yoon, and S. G. Louie, Physical Review Letters **83**, 5098 (1999).
[5] A. Bachtold, C. Strunk, J.-P. Salvetat, J.-M. Bonard, L. Forro, T. Nussbaumer, and C. Schonenberger, Nature **397**, 673 (1999).
[6] A. H. Castro Neto, F. Guinea, N. M. R. Peres, K. S. Novoselov, and A. K. Geim, Review of Modern Physics **81**, 109 (2009).
[7] S. Das Sarma, S. Adam, E. H. Hwang, and E. Rossi, Reviews of Modern Physics **83**, 407 (2011).
[8] J. H. Bardarson and J. E. Moore, Reports on Progress in Physics **76**, 056601 (2013).
[9] E. H. Hwang and S. Das Sarma, Physical Review B **77**, 195412 (2008).
[10] D. Culcer, E. H. Hwang, T. D. Stanescu, and S. Das Sarma, Physical Review B **82**, 155457 (2010).
[11] M. Monteverde, C. Ojeda-Aristizabal, R. Weil, K. Bennaceur, M. Ferrier, S. Guéron, C. Glattli, H. Bouchiat, J. N. Fuchs, and D. L. Maslov, Physical Review Letters **104**, 126801 (2010).
[12] J. Dufouleur, L. Veyrat, B. Dassonneville, C. Nowka, S. Hampel, P. Leksin, B. Eichler, O. G. Schmidt, B. Büchner, and R. Giraud, Nano Letters **16**, 6733 (2016).
[13] J. Tworzydlo, B. Trauzettel, M. Titov, A. Rycerz, and C. W. J. Beenakker, Physical Review Letters **96**, 246802 (2006).
[14] E. Prada, P. San-Jose, B. Wunsch, and F. Guinea, Physical Review B **75**, 113407 (2007).
[15] C. W. J. Beenakker, R. A. Sepkhanov, A. R. Akhmerov, and J. Tworzydlo, Physical Review Letters **102**, 146804 (2009).
[16] J. H. Bardarson, P. W. Brouwer, and J. E. Moore, Physical Review Letters **105**, 156803 (2010).
[17] Y. Zhang and A. Vishwanath, Physical Review Letters **105**, 206601 (2010).
[18] S. S. Hong, Y. Zhang, J. J. Cha, X.-L. Qi, and Y. Cui, Nano Letters **14**, 2815 (2014).
[19] S. Cho, B. Dellabetta, R. Zhong, J. Schneeloch, T. Liu, G. Gu, M. J. Gilbert, and N. Mason, Nature Communi-

cation **6**, (2015).
[20] Y.-M. Lin, V. Perebeinos, Z. Chen, and P. Avouris, Physical Review B **78**, 161409(R) (2008).
[21] N. Tombros, A. Veligura, J. Junesch, M. H. D. Guimaraes, I. J. Vera-Marun, H. T. Jonkman, and B. J. van Wees, Nature Physics **7**, 697 (2011).
[22] B. Terres, L. A. Chizhova, F. Libisch, J. Peiro, D. Jorger, S. Engels, A. Girschik, K. Watanabe, T. Taniguchi, S. V. Rotkin, J. Burgdorfer, and C. Stampfer, Nature Communications **7**, (2016).
[23] H. Peng, K. Lai, D. Kong, S. Meister, Y. Chen, X.-L. Qi, S.-C. Zhang, Z.-X. Shen, and Y. Cui, Nature Materials **9**, 225 (2010).
[24] F. Xiu, L. He, Y. Wang, L. Cheng, L.-T. Chang, M. Lang, G. Huang, X. Kou, Y. Zhou, X. Jiang, Z. Chen, J. Zou, A. Shailos, and K. L. Wang, Nature Nanotechnology **6**, 216 (2011).
[25] J. Dufouleur, L. Veyrat, A. Teichgräber, S. Neuhaus, C. Nowka, S. Hampel, J. Cayssol, J. Schumann, B. Eichler, O. G. Schmidt, B. Büchner, and R. Giraud, Physical Review Letters **110**, 186806 (2013).
[26] L. A. Jauregui, M. T. Pettes, L. P. Rokhinson, L. Shi, and Y. P. Chen, Nature Nanotechnology **11**, 345 (2016).
[27] J. Dufouleur, L. Veyrat, B. Dassonneville, E. Xypakis, J. H. Bardarson, C. Nowka, S. Hampel, J. Schumann, B. Eichler, O. G. Schmidt, B. Büchner, and R. Giraud, Scientific Reports **7**, 45276 (2017).
[28] Y. Xia, D. Qian, D. Hsieh, L. Wray, A. Pal, H. Lin, A. Bansil, D. Grauer, Y. S. Hor, R. J. Cava, and M. Z. Hasan, Nature Physics **5**, 398 (2009).
[29] Y. Zhang, Y. Ran, and A. Vishwanath, Physical Review B **79**, 245331 (2009).
[30] G. Rosenberg, H. M. Guo, and M. Franz, Physical Review B **82**, 041104 (2010).
[31] P. M. Ostrovsky, I. V. Gornyi, and A. D. Mirlin, Physical Review Letters **105**, 036803 (2010).
[32] S. Adam, P. W. Brouwer, and S. Das Sarma, Physical Review B **79**, 201404(R) (2009).
[33] In agreement with[32], we found a difference of a factor 4 with respect to the expression of ℓ written in[16].
[34] M. I. Katsnelson, K. S. Novoselov, and A. K. Geim, Nature Physics **2**, 620 (2006).
[35] R. Shankar, *Principles of Quantum Mechanics*, 2nd ed. (Springer US, 1994).
[36] T. Ando and H. Suzuura, Journal of the Physical Society of Japan **71**, 2753 (2002).
[37] J. H. Bardarson, Journal of Physics A: Mathematical and Theoretical **41**, 405203 (2008).
[38] J. H. Bardarson, J. Tworzydlo, P. W. Brouwer, and C. W. J. Beenakker, Physical Review Letters **99**, 106801 (2007).
[39] E. Xypakis and J. H. Bardarson, Physical Review B **95**, 035415 (2017).
[40] J. P. Robinson and H. Schomerus, Physical Review B **76**, 115430 (2007).
[41] Y. M. Blanter and I. Martin, Physical Review B **76**, 155433 (2007).
[42] A. Pieper, G. Schubert, G. Wellein, and H. Fehske, Physical Review B **88**, 195409 (2013).
[43] The differences between massless and massive particles is emphasized by the energy dependence of $\ell(\varepsilon)$. Indeed, $\ell > \ell_{\mathrm{m}}$ for massless particles and quantum confinement can be ensured for the full energy scale. On the contrary, for massive particles $\ell \to 0$ when $\varepsilon \to 0$ and overlapping cannot be avoided in the low energy limit.

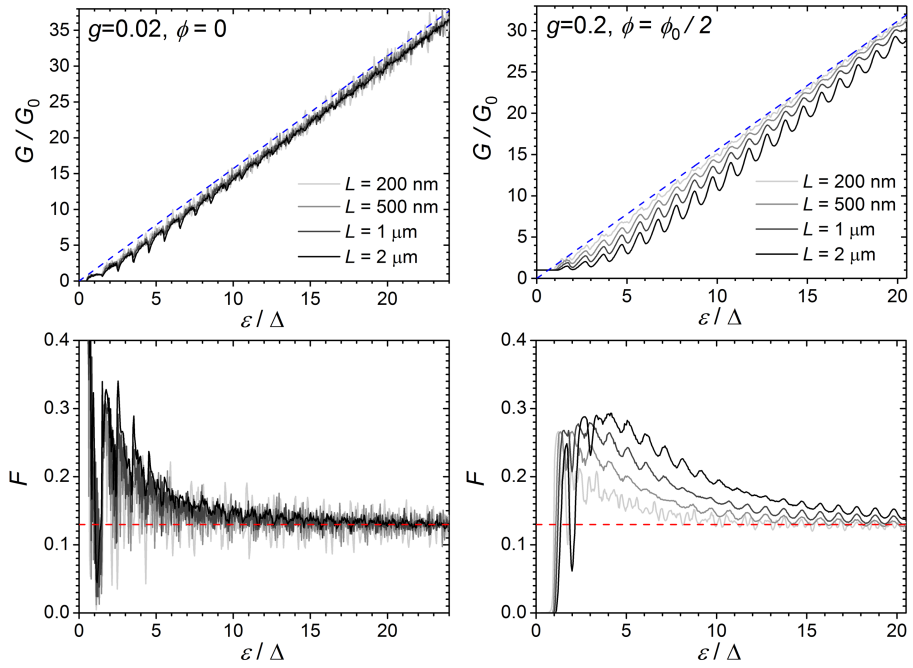

FIG. 9. Left: conductance and Fano factor ($g = 0.02$, $W = 200nm$, $\xi = 10nm$) for different wire lengths L. The large number of modes limit is indicated by the red dashed line. Right: conductance and Fano factor ($g = 0.2$, $W = 200nm$, $\xi = 10nm$) for different length. The large number of mode limit is indicated by the blue (conductance) and red (Fano factor) dashed lines.